

# Comparison of Belief Propagation and Iterative Threshold Decoding based on Dynamical Systems

Mohamad Mostafa, Werner G. Teich, Jürgen Lindner

Institute of Communications Engineering

Ulm University

Albert-Einstein-Allee 43, D-89081 Ulm, Germany

Email: mohamad.mostafa@uni-ulm.de

**Abstract**—For a special class of convolutional codes, iterative threshold decoding (ITD) has been shown by simulations to achieve the same error rate performance as belief propagation (BP). In order to get a better understanding of these iterative decoding algorithms, we describe ITD and BP as discrete-time dynamical systems. Based on the theory of dynamical systems, we compare the dynamical behavior of ITD and BP. For the special case of a linear dynamical system, the behavior can be completely characterized. In this case we show that the fixed points of both ITD and BP are globally stable but they do not coincide. The analysis is extended to the case of a continuous-time dynamical system, which represents an important step for modeling analog iterative decoders.

**Index Terms**—Belief propagation, iterative threshold decoding, dynamical systems, stability analysis, analog decoding.

## I. INTRODUCTION

Turbo codes and low-density parity-check (LDPC) codes have been shown to achieve an error rate performance very close to the Shannon limit [1]. Both are decoded iteratively. In order to achieve a better understanding of these powerful error correcting codes, iterative decoding algorithms have been considered as nonlinear dynamical systems and have been investigated using the well-established theory of nonlinear dynamical systems [2], [3].

As an example, it has been shown in [2] that a whole range of phenomena known to occur in nonlinear systems, such as existence of multiple fixed points, oscillatory behavior, bifurcation, chaos, and transient chaos are found in iterative decoding algorithms.

Improving the power/speed ratio has motivated the design of iterative decoders in the continuous-time domain (analog decoding). For this reason, several proof-of-concept analog decoders for short codes have been implemented. The continuous-time iterative decoder has been modeled as a first order nonlinear differential equation [4], [5], [6], [7]. It has been shown in [8] that the analog min-sum iterative decoder in the log-likelihood ratio (LLR) domain can be considered as a piecewise linear system.

Belief propagation (BP) arises in the context of iterative decoding of LDPC codes. In a series of papers [9], [10], [11], [12] it has been shown that the less complex iterative threshold decoding (ITD) achieves the same error rate performance as BP for a special class of convolutional codes, namely convolutional self (and self-doubly) orthogonal codes.

In contrast to BP, the dynamical behavior of ITD has not attracted that amount of attention. This is investigated in this paper for both discrete-time and continuous-time cases. The connection between ITD and high order recurrent neural networks has already been investigated [13].

The behavior of BP as a linear discrete-time dynamical system has been investigated in [3]. In this paper, we extend this analysis to the continuous-time case on one hand and we compare it with ITD for both discrete and continuous-time cases on the other hand. We show that the discrete-time dynamical model proposed for BP in [3] is valid for ITD too.

The following notation is used throughout the paper. Vectors are underlined once, matrices twice.  $(\cdot)^T$  denotes the transpose of a matrix or a vector.  $|\cdot|$ ,  $\Re\{\cdot\}$ ,  $\Im\{\cdot\}$  denote the absolute, real and imaginary value of a scalar, respectively.  $\underline{I}_{a \times a}$ ,  $\underline{1}_{a \times b}$ ,  $\underline{0}_{a \times b}$  denote an identity matrix of size  $a \times a$ , a matrix of ones of size  $a \times b$ , and a zero matrix of size  $a \times b$ , respectively.  $\text{eig}\{\cdot\}$  returns the eigenvalues of the matrix in the argument.

The paper is organized as follows: We begin in Section II with the definition of the transmission model. In Section III we introduce dynamical systems. The core of this section is the definition of the so called "twin dynamical systems". In Section IV we formulate BP and ITD as dynamical systems and we investigate their (global) stability in the linear case in Section V. We finish with the conclusion in Section VI.

## II. TRANSMISSION MODEL

Every binary linear block code  $(n, k, d)$  is characterized by a (binary) parity check matrix  $\underline{H}$  of size  $(n - k) \times n$  [14].

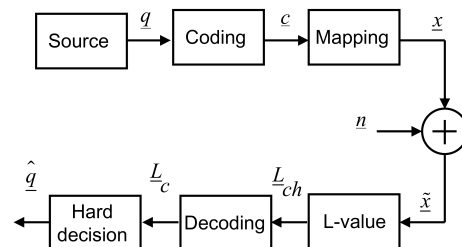


Fig. 1. Transmission over a discrete-time AWGN channel,  $q$  is the information word,  $c$  the codeword,  $x$  the transmitted word,  $n$  white noise samples,  $\tilde{x}$  the received word,  $L_{ch}$  the intrinsic L-Values,  $L_c$ , the L-values of the code symbols after the decoding process and  $\tilde{q}$  the hard decision.

$k, n, d$ : The length of the information word, the length of the codeword, and the minimum Hamming distance of the code. In Fig. 1 a codeword  $\underline{c} = (c_1, c_2, \dots, c_n)$ ,  $c_i \in \{0, 1\}$  is transmitted after mapping it to antipodal symbols over a discrete-time additive white Gaussian noise (AWGN) channel. The received word  $\tilde{x} = (\tilde{x}_1, \tilde{x}_2, \dots, \tilde{x}_n)$  is the input of the (soft) decoding algorithm.  $\underline{L}_c = (L_c^{(1)}, L_c^{(2)}, \dots, L_c^{(n)})$  is the vector of the log-likelihood values (L-value) of the code symbols after the decoding process.

### III. DYNAMICAL SYSTEMS

#### A. Definitions

We describe a discrete-time dynamical system (DTDS) by equations of the form

$$\underline{x}(l+1) = \underline{s}[\underline{x}(l)] \quad , \quad \underline{x}(0) = \underline{x}_0 \quad , \quad l = 0, 1, 2, \dots \quad (1)$$

and a continuous-time dynamical system (CTDS) by:

$$\underline{\tau} \cdot \frac{d\underline{x}(t)}{dt} = \underline{g}[\underline{x}(t)] \quad , \quad \underline{x}(0) = \underline{x}_0 \quad , \quad t \geq 0 \quad (2)$$

where  $\underline{s}$  and  $\underline{g}$  are in general complex-valued and partially continuously differentiable functions and  $\underline{x} \in \mathbb{C}^N$ .  $\underline{\tau}$  is a diagonal positive definite matrix.

The fixed points  $\underline{x}_{fp}$  of the DTDS in Eq. (1) fulfill:

$$\underline{x}_{fp} = \underline{s}[\underline{x}_{fp}]. \quad (3)$$

The equilibrium points  $\underline{x}_{ep}$  of the CTDS in Eq. (2) fulfill:

$$\underline{g}[\underline{x}_{ep}] = \underline{0}. \quad (4)$$

#### B. The Linear Case

This subsection is based mainly on [15].

**Discrete-Time Case:** In case of a linear DTDS:

$$\underline{x}(l+1) = \underline{D} \cdot \underline{x}(l) + \underline{d} \quad , \quad \underline{x}(0) = \underline{x}_0 \quad , \quad l = 0, 1, 2, \dots \quad (5)$$

The system possesses only one fixed point if  $[\underline{I} - \underline{D}]$  is non-singular. In this case:

$$\underline{x}_{fp} = -[\underline{D} - \underline{I}]^{-1} \cdot \underline{d}. \quad (6)$$

$\underline{x}_{fp}$  is globally stable if:

$$\forall i \in \{1, 2, \dots, N\} : |\lambda_{\underline{D}}^{(i)}| < 1. \quad (7)$$

where  $\lambda_{\underline{D}}^{(i)}$  represents the i-th eigenvalue of  $\underline{D}$ .

**Continuous-Time Case:** For the linear CTDS:

$$\underline{\tau} \cdot \frac{d\underline{x}(t)}{dt} = \underline{C} \cdot \underline{x}(t) + \underline{c} \quad , \quad \underline{x}(0) = \underline{x}_0 \quad , \quad t \geq 0 \quad (8)$$

The system possesses only one equilibrium point if  $\underline{C}$  is non-singular. In this case:

$$\underline{x}_{ep} = -\underline{C}^{-1} \cdot \underline{c}. \quad (9)$$

$\underline{x}_{ep}$  is globally stable if:

$$\forall i \in \{1, 2, \dots, N\} : \Re \left\{ \lambda_{\underline{C}}^{(i)} \right\} < 0. \quad (10)$$

where  $\lambda_{\underline{C}}^{(i)}$  represents the i-th eigenvalue of  $\underline{C}$ .

If  $\underline{D} - \underline{I}$  and  $\underline{C}$  are nonsingular and Eq. (7),(10) are fulfilled, the linear dynamical systems described in Eq. (5),(8) will asymptotically reach  $\underline{x}_{fp}$  and  $\underline{x}_{ep}$  in Eq. (6),(9), respectively, regardless of the initial condition  $\underline{x}_0$  (global stability).

#### C. Twin Dynamical Systems

We are interested in defining CTDSs that deliver similar solutions to those given by DTDSs. This means, we want to define  $\underline{g}$  in Eq. (2) in terms of  $\underline{s}$  in Eq. (1) such that both systems in Eq. (1),(2) share specific characteristics. To do that we have to make further restrictions, namely:

- 1) The DTDS and the CTDS share the same set of fixed/equilibrium points.
- 2) If a fixed point of the DTDS is stable then it must be stable in the CTDS too.

One possible solution to fulfill these conditions for the linear case is:

$$\underline{c} = \underline{d} \quad , \quad \underline{C} = -\underline{I} + \underline{D} \quad (11)$$

This means:  $\forall i \in \{1, 2, \dots, N\}$ :

$$\Re \left\{ \lambda_{\underline{C}}^{(i)} \right\} = -1 + \Re \left\{ \lambda_{\underline{D}}^{(i)} \right\} \quad , \quad \Im \left\{ \lambda_{\underline{C}}^{(i)} \right\} = \Im \left\{ \lambda_{\underline{D}}^{(i)} \right\} \quad (12)$$

If the linear DTDS is globally stable, i.e. Eq. (7) is fulfilled, then according to Eq. (12):

$$\forall i \in \{1, 2, \dots, N\} : -2 < \Re \left\{ \lambda_{\underline{C}}^{(i)} \right\} < 0$$

We notice in this case that Eq. (10) is fulfilled and the linear CTDS is globally stable too. In this case Eq. (5),(8) can be rewritten as:

$$\begin{aligned} \underline{x}(l+1) &= \underline{D} \cdot \underline{x}(l) + \underline{d} \\ \underline{\tau} \cdot \frac{d\underline{x}(t)}{dt} &= -\underline{x}(t) + \underline{D} \cdot \underline{x}(t) + \underline{d} \\ \underline{x}(0) &= \underline{x}_0 \quad \& \quad t \geq 0 \quad \& \quad l = 0, 1, 2, \dots \end{aligned} \quad (13)$$

One possible solution for the nonlinear dynamical systems Eq. (1),(2) is:

$$\underline{g}[\underline{x}] = -\underline{x} + \underline{s}[\underline{x}] \quad (14)$$

This means for the eigenvalues of the Jacobian matrices of  $\underline{s}$  and  $\underline{g}$ :

$$\underline{J}_{\underline{g}}[\underline{x}] = -\underline{I} + \underline{J}_{\underline{s}}[\underline{x}] \quad , \quad \underline{\lambda}_{\underline{J}_{\underline{g}}} = -\underline{I} + \underline{\lambda}_{\underline{J}_{\underline{s}}} \quad (15)$$

$\underline{J}_{\underline{g}}[\underline{x}]$ ,  $\underline{J}_{\underline{s}}[\underline{x}]$  are the Jacobian matrices of the functions  $\underline{g}$ ,  $\underline{s}$  respectively and  $\underline{\lambda}_{\underline{J}_{\underline{g}}}$ ,  $\underline{\lambda}_{\underline{J}_{\underline{s}}}$  are diagonal matrices and the diagonal elements are the eigenvalues of the Jacobian matrices of  $\underline{g}[\underline{x}]$  and  $\underline{s}[\underline{x}]$  respectively. We notice that Eq. (15) is the matrix-notation of Eq. (12). We can rewrite Eq. (1),(2) as follows:

$$\begin{aligned} \underline{x}(l+1) &= \underline{s}[\underline{x}(l)] \\ \underline{\tau} \cdot \frac{d\underline{x}(t)}{dt} &= -\underline{x}(t) + \underline{s}[\underline{x}(t)] \\ \underline{x}(0) &= \underline{x}_0 \quad \& \quad t \geq 0 \quad \& \quad l = 0, 1, 2, \dots \end{aligned} \quad (16)$$

**Definition 1:** If Eq. (14) is fulfilled, then the DTDS in Eq. (1) and the CTDS in Eq. (2) are twin.

**Remark 1:** Eq. (14) has been derived under the assumption that the linearization method is applicable.

**Remark 2:** Even if the CTDS and the DTDS are twin, the trajectory of the CTDS is generally not an interpolation of the trajectory of the DTDS.

### D. The Connection with Low Pass Filtering

The second line in Eq. (16) can be rewritten for the one dimensional case as follows:

$$\tau \cdot \frac{dx(t)}{dt} = -x(t) + s[x(t)] \quad (17)$$

This represents the behavior of a passive first order low pass filter. This fact motivated the modeling of analog iterative decoders in [4]–[8] by the second line in Eq. (16). By the definition of twin dynamical systems, we show that this model Eq. (16) has important dynamical properties as well.

### IV. ITERATIVE DECODING AS A DYNAMICAL SYSTEM

The parity check equations of binary linear block codes can be visualized in a very efficient way using Tanner graphs [16]. Furthermore, Tanner graphs give good insight into the code structure and the structure of iterative decoding algorithms. Tanner graph consists of two types of nodes, variable nodes and check nodes, connected to each other by edges. Each code symbol is represented by a variable node and each parity check equation is represented by a check node. A variable node, representing the  $i$ -th code symbol, is connected to a check node, representing the  $j$ -th parity check equation, if the  $i$ -th code symbol appears in the  $j$ -th parity check equation. Fig. 2 shows the Tanner graph of the systematic Hamming code (7,4,3) with the parity check matrix

$$\underline{\underline{H}} = \left[ \begin{array}{cccc|ccc} 0 & 1 & 1 & 1 & 1 & 0 & 0 \\ 1 & 0 & 1 & 1 & 0 & 1 & 0 \\ 1 & 1 & 0 & 1 & 0 & 0 & 1 \end{array} \right]$$

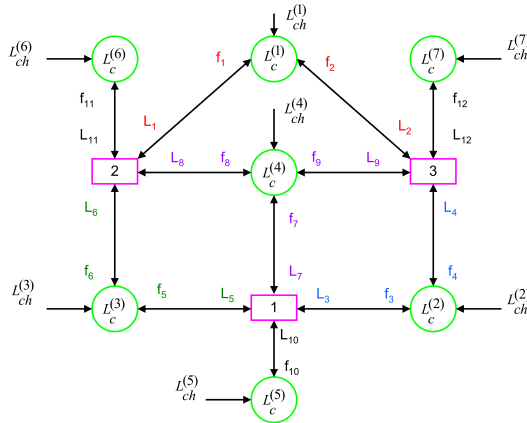


Fig. 2. Tanner graph of the systematic Hamming code (7,4,3).

Generally, we define:

$$\begin{aligned} \underline{L}_{ch} &= \left[ L_{ch}^{(1)}, L_{ch}^{(2)}, \dots, L_{ch}^{(n)} \right]^T & \underline{f} &= [f_1, f_2, \dots, f_r]^T \\ \underline{L}_c &= \left[ L_c^{(1)}, L_c^{(2)}, \dots, L_c^{(n)} \right]^T & \underline{L} &= [L_1, L_2, \dots, L_r]^T \end{aligned} \quad (18)$$

$r$  is the number of edges in the Tanner graph, which equals the number of the nonzero entries in the parity check matrix.  $\underline{L}$  is the vector of L-values sent from the variable nodes to the

check nodes depending on the iterative decoding algorithm.  $\underline{f}$  is the vector of L-values sent from the check nodes to the variable nodes (extrinsic L-values) depending on the iterative decoding algorithm. In details,  $f_i$  which is emerging from the  $v$ -th check node to the  $y$ -th variable node depends on all L-values arriving at the  $v$ -th check nodes except that L-value emerging from the  $y$ -th variable node ( $L_i$ ). As an example,  $f_1$  in Fig. 2 is a function of  $L_6, L_8, L_{11}$ .

$\underline{L}_{ch}$  is the vector of intrinsic L-values, which depend on the transition probability of the channel. For an AWGN channel and antipodal modulation:

$$L_{ch}^{(i)} = \frac{2 \cdot \tilde{x}_i}{\sigma^2} \quad (19)$$

$\sigma^2$  is the noise power.

$\underline{L}_c$  is the vector of the L-values of the code symbols after the decoding process (soft decision).

Enumerating the entries in Eq. (18) has been done in a symbol-ascending order and for each symbol in an ascending order depending on the check nodes.

Iterative decoding algorithms depend on the iterative exchange of L-values between the variable and the check nodes as illustrated in Fig. 3, where  $l$  is the discrete-time index.

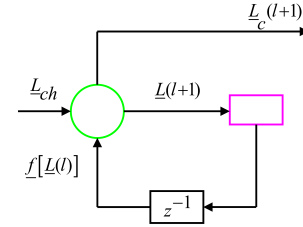


Fig. 3. Iterative decoding as a discrete-time dynamical system.

In the following we specify the structure in Fig. 3 in detail for both iterative decoding approaches, namely BP and ITD. For this purpose we define the following binary matrices:  $\underline{\underline{S}}_{r \times r}$ ,  $\underline{\underline{P}}_{r \times r}$ ,  $\underline{\underline{B}}_{r \times n}$ . These definition are slightly different from those in [3].

$$\underline{\underline{S}}_{r \times r} = \{S_{ij} \in \{0, 1\} : \forall i, j \in \{1, 2, \dots, r\}\}:$$

$$S_{ij} = \begin{cases} 1 & f_i \text{ is a function of } L_j \\ 0 & \text{otherwise} \end{cases}$$

For example, the first row of  $\underline{\underline{S}}$  for the code given in Fig. 2 is  $[0 \ 0 \ 0 \ 0 \ 0 \ 1 \ 0 \ 1 \ 0 \ 0 \ 1 \ 0]$  and

$$f_i = 2 \cdot \text{atanh} \left\{ \prod_{j \in \text{pos}[\underline{\underline{S}}(i, :) \neq 0]} \tanh \left[ \frac{L_j}{2} \right] \right\} \quad (20)$$

$\text{pos}[\underline{\underline{S}}(i, :) \neq 0]$  gives the positions of the nonzero elements in the  $i$ -th row of  $\underline{\underline{S}}$ .

$\underline{\underline{P}}_{r \times r}$ :  $\forall i, j \in \{1, 2, \dots, r\}$  imagine that the  $i$ -th row in  $\underline{\underline{P}}$  represents  $L_i$ , where the  $j$ -th column represents  $f_j$ . For each  $L_i$  emerging from the  $y$ -th variable node to the  $v$ -th check node, the  $i$ -th row (representing  $L_i$ ) contains nonzero

elements (ones) in that columns  $j$  representing all  $f_j$  arriving at the  $y$ -th variable node except  $f_i$ . For example, the seventh row of  $\underline{\underline{P}}$  (representing  $L_7$ ) for the code given in Fig. 2 is  $[0 \ 0 \ 0 \ 0 \ 0 \ 0 \ 0 \ 0 \ 1 \ 1 \ 0 \ 0 \ 0]^T$ .

$\underline{\underline{B}}_{r \times n} : \forall j \in \{1, 2, \dots, n\}$  the number of nonzero elements in the  $j$ -th column equals to the number of nonzero elements in the  $j$ -th column of the parity check matrix. Each row contains only one nonzero element. For example, the first and second columns of  $\underline{\underline{B}}$  for the code given in Fig. 2 are 
$$\begin{bmatrix} 1 & 1 & 0 & 0 & 0 & 0 & 0 & 0 & 0 & 0 & 0 & 0 \\ 0 & 0 & 1 & 1 & 0 & 0 & 0 & 0 & 0 & 0 & 0 & 0 \end{bmatrix}^T$$

#### A. The Dynamical System of BP

In the discrete-time case:

$$\begin{aligned} \underline{L}(l+1) &= \underline{\underline{P}} \cdot \underline{f}[\underline{L}(l)] + \underline{\underline{B}} \cdot \underline{L}_{ch} \\ \underline{L}_c(l+1) &= \underline{\underline{B}}^T \cdot \underline{f}[\underline{L}(l)] + \underline{L}_{ch} \end{aligned} \quad (21)$$

This has already been described in [3].

In the continuous-time case according to Eq. (16):

$$\begin{aligned} \underline{\tau} \cdot \frac{d\underline{L}(t)}{dt} &= -\underline{L}(t) + \underline{\underline{P}} \cdot \underline{f}[\underline{L}(t)] + \underline{\underline{B}} \cdot \underline{L}_{ch} \\ \underline{L}_c(t) &= \underline{\underline{B}}^T \cdot \underline{f}[\underline{L}(t)] + \underline{L}_{ch} \end{aligned} \quad (22)$$

#### B. The Dynamical System of ITD

In the discrete-time case:

$$\begin{aligned} \underline{L}(l+1) &= \underline{\underline{w}}_1 \cdot \underline{\underline{A}} \cdot \underline{\underline{B}} \cdot \underline{\underline{B}}^T \cdot \underline{f}[\underline{L}(l)] + \underline{\underline{w}}_0 \cdot \underline{\underline{B}} \cdot \underline{L}_{ch} \\ \underline{L}_c(l+1) &= \underline{\underline{B}}^T \cdot \underline{f}[\underline{L}(l)] + \underline{L}_{ch} \end{aligned} \quad (23)$$

In the continuous-time case according to Eq. (16):

$$\begin{aligned} \underline{\tau} \cdot \frac{d\underline{L}(t)}{dt} &= -\underline{L}(t) + \underline{\underline{w}}_1 \cdot \underline{\underline{A}} \cdot \underline{\underline{B}} \cdot \underline{\underline{B}}^T \cdot \underline{f}[\underline{L}(t)] \\ &\quad + \underline{\underline{w}}_0 \cdot \underline{\underline{B}} \cdot \underline{L}_{ch} \\ \underline{L}_c(t) &= \underline{\underline{B}}^T \cdot \underline{f}[\underline{L}(t)] + \underline{L}_{ch} \end{aligned} \quad (24)$$

In Eq. (23), (24):

$$\begin{aligned} \underline{\underline{w}}_1 &= \left[ \begin{array}{c|c} \underline{\underline{w}}_1^{ul} & \underline{\underline{0}}_{(r-m) \times m} \\ \hline \underline{\underline{0}}_{m \times (r-m)} & \underline{\underline{0}}_{m \times m} \end{array} \right] \\ \underline{\underline{w}}_0 &= \left[ \begin{array}{c|c} \underline{\underline{w}}_0^{ul} & \underline{\underline{0}}_{(r-m) \times m} \\ \hline \underline{\underline{0}}_{m \times (r-m)} & \underline{\underline{w}}_0^{br} \end{array} \right] \end{aligned} \quad (25)$$

where  $m = n - k$  and  $\underline{\underline{w}}_1^{ul} = \text{diag} \{ \underline{\underline{w}}_1^{ul} \}$ ,  $\underline{\underline{w}}_0^{ul} = \text{diag} \{ \underline{\underline{w}}_0^{ul} \}$ ,  $\underline{\underline{w}}_0^{br} = \text{diag} \{ \underline{\underline{w}}_0^{br} \}$ .

$$\begin{aligned} \underline{\underline{w}}_1^{ul} &= [w_{1,1}, w_{2,1}, \dots, w_{r-m,1}]^T \\ \underline{\underline{w}}_0^{ul} &= [w_{1,0}, w_{2,0}, \dots, w_{r-m,0}]^T \\ \underline{\underline{w}}_0^{br} &= [w_{r-m+1,0}, w_{r-m+2,0}, \dots, w_{r,0}]^T \end{aligned}$$

The nonzero entries in  $\underline{\underline{w}}_0$ ,  $\underline{\underline{w}}_1$  are positive.  $\underline{\underline{w}}_0$ ,  $\underline{\underline{w}}_1$  represent the matrices of weight factors, which are usually optimized by simulations. In addition:

$$\underline{\underline{A}} = \left[ \begin{array}{c|c} \underline{\underline{I}}_{(r-m) \times (r-m)} & \underline{\underline{0}}_{(r-m) \times m} \\ \hline \underline{\underline{0}}_{m \times (r-m)} & \underline{\underline{0}}_{m \times m} \end{array} \right] \quad (26)$$

## V. STABILITY ANALYSIS IN THE LINEAR CASE

If each row of the parity check matrix contains exactly two nonzero elements, then every check node in the Tanner graph of the corresponding code is connected with two variable nodes. In this special case, every row in the matrix  $\underline{\underline{S}}$  contains only one nonzero element and becomes a permutation matrix. In this case Eq. (20) can be rewritten as:  $f_i = L_j$ . This has already been found in [3]. In this case Eq. (21), (22), (23), (24) can be rewritten as:

#### A. BP

**Discrete-time:**

$$\begin{aligned} \underline{L}(l+1) &= \underline{\underline{P}} \cdot \underline{\underline{S}} \cdot \underline{L}(l) + \underline{\underline{B}} \cdot \underline{L}_{ch} \\ \underline{L}_c(l+1) &= \underline{\underline{B}}^T \cdot \underline{\underline{S}} \cdot \underline{L}(l) + \underline{L}_{ch} \end{aligned} \quad (27)$$

**Continuous-time:**

$$\begin{aligned} \underline{\tau} \cdot \frac{d\underline{L}(t)}{dt} &= -\underline{L}(t) + \underline{\underline{P}} \cdot \underline{\underline{S}} \cdot \underline{L}(t) + \underline{\underline{B}} \cdot \underline{L}_{ch} \\ \underline{L}_c(t) &= \underline{\underline{B}}^T \cdot \underline{\underline{S}} \cdot \underline{L}(t) + \underline{L}_{ch} \end{aligned} \quad (28)$$

The stability in this case depends on the eigenvalues of  $\underline{\underline{P}} \cdot \underline{\underline{S}}$  where  $\underline{\underline{I}} - \underline{\underline{P}} \cdot \underline{\underline{S}}$  is nonsingular.

**Fixed/Equilibrium Points:**

$$\begin{aligned} \underline{L}_{fp} = \underline{L}_{ep} &= [\underline{\underline{I}} - \underline{\underline{P}} \cdot \underline{\underline{S}}]^{-1} \cdot \underline{\underline{B}} \cdot \underline{L}_{ch} \\ \underline{L}_{c,fp} = \underline{L}_{c,ep} &= \left\{ \underline{\underline{B}}^T \cdot \underline{\underline{S}} \cdot [\underline{\underline{I}} - \underline{\underline{P}} \cdot \underline{\underline{S}}]^{-1} \cdot \underline{\underline{B}} + \underline{\underline{I}} \right\} \cdot \underline{L}_{ch} \end{aligned} \quad (29)$$

#### B. ITD

**Discrete-time:**

$$\begin{aligned} \underline{L}(l+1) &= \underline{\underline{w}}_1 \cdot \underline{\underline{A}} \cdot \underline{\underline{B}} \cdot \underline{\underline{B}}^T \cdot \underline{\underline{S}} \cdot \underline{L}(l) + \underline{\underline{w}}_0 \cdot \underline{\underline{B}} \cdot \underline{L}_{ch} \\ \underline{L}_c(l+1) &= \underline{\underline{B}}^T \cdot \underline{\underline{S}} \cdot \underline{L}(l) + \underline{L}_{ch} \end{aligned} \quad (30)$$

**Continuous-time:**

$$\begin{aligned} \underline{\tau} \cdot \frac{d\underline{L}(t)}{dt} &= -\underline{L}(t) + \underline{\underline{w}}_1 \cdot \underline{\underline{A}} \cdot \underline{\underline{B}} \cdot \underline{\underline{B}}^T \cdot \underline{\underline{S}} \cdot \underline{L}(t) \\ &\quad + \underline{\underline{w}}_0 \cdot \underline{\underline{B}} \cdot \underline{L}_{ch} \\ \underline{L}_c(t) &= \underline{\underline{B}}^T \cdot \underline{\underline{S}} \cdot \underline{L}(t) + \underline{L}_{ch} \end{aligned} \quad (31)$$

The stability in this case depends on the eigenvalues of  $\underline{\underline{w}}_1 \cdot \underline{\underline{A}} \cdot \underline{\underline{B}} \cdot \underline{\underline{B}}^T \cdot \underline{\underline{S}}$  where  $\underline{\underline{I}} - \underline{\underline{w}}_1 \cdot \underline{\underline{A}} \cdot \underline{\underline{B}} \cdot \underline{\underline{B}}^T \cdot \underline{\underline{S}}$  is nonsingular.

**Fixed/Equilibrium Points:**

$$\begin{aligned} \underline{L}_{fp} = \underline{L}_{ep} &= [\underline{\underline{I}} - \underline{\underline{w}}_1 \cdot \underline{\underline{A}} \cdot \underline{\underline{B}} \cdot \underline{\underline{B}}^T \cdot \underline{\underline{S}}]^{-1} \cdot \underline{\underline{w}}_0 \cdot \underline{\underline{B}} \cdot \underline{L}_{ch} \\ \underline{L}_{c,fp} = \underline{L}_{c,ep} &= \\ \underline{\underline{B}}^T \cdot \underline{\underline{S}} \cdot [\underline{\underline{I}} - \underline{\underline{w}}_1 \cdot \underline{\underline{A}} \cdot \underline{\underline{B}} \cdot \underline{\underline{B}}^T \cdot \underline{\underline{S}}]^{-1} &\cdot \underline{\underline{w}}_0 \cdot \underline{\underline{B}} \cdot \underline{L}_{ch} + \underline{L}_{ch} \end{aligned} \quad (32)$$

## C. Repetition Codes

The generator and parity check matrices of repetition codes with  $n$  code symbols,  $k = 1$  information symbol, and  $m = n - 1$  parity check symbols are given as follows:

$$\underline{G}_{1 \times n} = \begin{bmatrix} 1 & | & \underline{1}_{1 \times m} \end{bmatrix}, \quad \underline{H}_{m \times n} = \begin{bmatrix} \underline{1}_{m \times 1} & | & \underline{I}_{m \times m} \end{bmatrix} \quad (33)$$

We notice that every row of the parity check matrix contains exactly two non-zero elements and  $r = 2 \cdot m$ , ( $r - m = m$ ). In this case it can be shown that:

$$\begin{aligned} \underline{P} &= \begin{bmatrix} (\underline{1} - \underline{I})_{m \times m} & | & \underline{0}_{m \times m} \\ \underline{0}_{m \times m} & | & \underline{0}_{m \times m} \end{bmatrix}, \quad \underline{S} = \begin{bmatrix} \underline{0}_{m \times m} & | & \underline{I}_{m \times m} \\ \underline{I}_{m \times m} & | & \underline{0}_{m \times m} \end{bmatrix} \\ \underline{B} &= \begin{bmatrix} \underline{1}_{m \times 1} & | & \underline{0}_{m \times m} \\ \underline{0}_{m \times 1} & | & \underline{I}_{m \times m} \end{bmatrix}, \quad \underline{P} \cdot \underline{S} = \begin{bmatrix} \underline{0}_{m \times m} & | & (\underline{1} - \underline{I})_{m \times m} \\ \underline{0}_{m \times m} & | & \underline{0}_{m \times m} \end{bmatrix} \\ [\underline{I} - \underline{P} \cdot \underline{S}]^{-1} &= \begin{bmatrix} \underline{I}_{m \times m} & | & (\underline{1} - \underline{I})_{m \times m} \\ \underline{0}_{m \times m} & | & \underline{I}_{m \times m} \end{bmatrix} \end{aligned} \quad (34)$$

The eigenvalues of a triangular matrix are the elements on the main diagonal [17] i.e. the eigenvalues of  $\underline{P} \cdot \underline{S}$  are 0 with multiplicity  $2 \cdot m$ . This leads to the fact that BP for repetition codes is always stable in both discrete and continuous-time cases. Using Eq. (34) it can be found that

$$\underline{B}^T \cdot \underline{S} \cdot [\underline{I} - \underline{P} \cdot \underline{S}]^{-1} \cdot \underline{B} + \underline{I} = \underline{1}_{n \times n} \quad (35)$$

Thus Eq. (29) can be rewritten as:

$$\underline{L}_{c,fp} = \underline{L}_{c,ep} = \underline{1}_{n \times n} \cdot \underline{L}_{ch} \quad (36)$$

This has been shown in [3] for the discrete-time case. Here, we have proved it using the detailed structures of  $\underline{S}$ ,  $\underline{P}$ , and  $\underline{B}$ . In addition, we generalized this result to the continuous-time case.

Furthermore, it can be shown that:

$$\begin{aligned} \underline{w}_1 \cdot \underline{A} \cdot \underline{B} \cdot \underline{B}^T \cdot \underline{S} &= \begin{bmatrix} \underline{0}_{m \times m} & | & \underline{w}_1^{ul} \cdot \underline{1}_{m \times m} \cdot \underline{1}_{m \times m} \\ \underline{0}_{m \times m} & | & \underline{0}_{m \times m} \end{bmatrix} \\ [\underline{I} - \underline{w}_1 \cdot \underline{A} \cdot \underline{B} \cdot \underline{B}^T \cdot \underline{S}]^{-1} &= \begin{bmatrix} \underline{I}_{m \times m} & | & \underline{w}_1^{ul} \cdot \underline{1}_{m \times m} \cdot \underline{1}_{m \times m} \\ \underline{0}_{m \times m} & | & \underline{I}_{m \times m} \end{bmatrix} \end{aligned} \quad (37)$$

Again, the eigenvalues of  $\underline{w}_1 \cdot \underline{A} \cdot \underline{B} \cdot \underline{B}^T \cdot \underline{S}$  are 0 with multiplicity  $2 \cdot m$ . We conclude that ITD for repetition codes is always stable for both discrete and continuous-time cases. Depending on Eq. (25),(26),(34) it can be found that:

$$\begin{aligned} \underline{B}^T \cdot \underline{S} \cdot [\underline{I} - \underline{w}_1 \cdot \underline{A} \cdot \underline{B} \cdot \underline{B}^T \cdot \underline{S}]^{-1} \cdot \underline{w}_0 \cdot \underline{B} + \underline{I} &= \\ \begin{bmatrix} 1 & | & \underline{w}_0^{br,T} \\ \underline{w}_0^{ul} & | & \underline{I} + \underline{w}_1^{ul} \cdot \underline{1} \cdot \underline{w}_0^{br} \end{bmatrix} \end{aligned} \quad (38)$$

and

$$\underline{L}_{c,fp} = \underline{L}_{c,ep} = \begin{bmatrix} 1 & | & \underline{w}_0^{br,T} \\ \underline{w}_0^{ul} & | & \underline{I} + \underline{w}_1^{ul} \cdot \underline{1} \cdot \underline{w}_0^{br} \end{bmatrix} \cdot \underline{L}_{ch} \quad (39)$$

We notice that the fixed points of BP and ITD do not coincide. In contrast to ITD, BP with repetition codes delivers maximum likelihood solutions (Tanner graph is a tree in this case).

## VI. CONCLUSION

In this paper we investigate the dynamics of belief propagation and iterative threshold decoding for the discrete and continuous-time case. We define also the continuous-time dynamics of these iterative decoding algorithms, which exhibit similar behavior near the fixed/equilibrium points. For repetition codes the dynamics of belief propagation and iterative threshold decoding is linear. In this case closed form results for the stability and fixed/equilibrium points have been derived and we show that belief propagation and iterative threshold decoding are always stable but they possess different fixed/equilibrium points.

## REFERENCES

- [1] S. J. Johnson, *Iterative error correction: Turbo, low-density parity-check and repeat-accumulate codes*. Cambridge University Press, 2010.
- [2] L. Kocarev, F. Lehmann, G. M. Maggio, B. Scanavino, Z. Tasev, and A. Vardy, "Nonlinear dynamics of iterative decoding systems: Analysis and applications," *IEEE Transactions on Information Theory*, vol. 52, no. 4, pp. 1366–1384, 2006.
- [3] B. S. Rüffer, C. M. Kellett, P. M. Dower, and S. R. Weller, "Belief propagation as a dynamical system: The linear case and open problems," *IET Control Theory Applications*, vol. 4, no. 7, pp. 1188–1200, 2010.
- [4] S. Hemati and A. H. Banihashemi, "Comparison between continuous-time asynchronous and discrete-time synchronous iterative decoding," in *IEEE Global Telecommunications Conference*, vol. 1, November/December 2004, pp. 356–360.
- [5] —, "Dynamics and performance analysis of analog iterative decoding for low-density parity-check (LDPC) codes," *IEEE Transactions on Communications*, vol. 54, no. 1, pp. 61–70, January 2006.
- [6] —, "Convergence speed and throughput of analog decoders," *IEEE Transactions on Communications*, vol. 55, no. 5, pp. 833–836, May 2007.
- [7] S. Hemati and A. Yongacoglu, "Dynamics of analog decoders for different message passing representation domains," *IEEE Transactions on Communications*, vol. 58, no. 3, pp. 721–723, May 2010.
- [8] —, "On the dynamics of analog min-sum iterative decoders: An analytical approach," *IEEE Transactions on Communications*, vol. 58, no. 8, pp. 2225–2231, August 2010.
- [9] W. G. Teich, "Iterative decoding of one-dimensional convolutional codes," in *4th International symposium on communication theory & applications in Ambleside, U.K.*, 13-18 July 1997, pp. 52–53.
- [10] C. Cardinal, D. Haccoun, and F. Gagnon, "Iterative threshold decoding without interleaving for convolutional self-doubly orthogonal codes," *IEEE Transactions on Communications*, vol. 51, no. 8, pp. 1274–1282, 2003.
- [11] C. Cardinal and D. Haccoun, "Convolutional self-doubly orthogonal codes and their iterative threshold decoding," in *Proceedings of the IEEE 15th International Symposium on Personal, Indoor and Mobile Radio Communications, PIMRC 2004, 5-8 September 2004, Barcelona, Spain*. IEEE, 2004.
- [12] Y.-C. He, D. Haccoun, and C. Cardinal, "Performance comparison of iterative BP and threshold decoding for convolutional self-doubly-orthogonal codes," in *VTC Spring*, 2007, pp. 2000–2004.
- [13] M. Mostafa, W. G. Teich, and J. Lindner, "Analysis of high order recurrent neural networks for analog decoding," in *7th international symposium on turbo codes and iterative information processing (ISTC)*, Gothenburg, Sweden, 27-31 August 2012, pp. 116–120.
- [14] M. Bossert, *Channel Coding for Telecommunications*. John Wiley & Sons Ltd, 1999.
- [15] E. R. Scheinerman, *Invitation to dynamical systems*. Prentice Hall, 1996.
- [16] R. Tanner, "A recursive approach to low complexity codes," *IEEE Transactions on Information Theory*, vol. 27, no. 5, pp. 533–547, September 1981.
- [17] A. Quarteroni, R. Sacco, and F. Saleri, *Numerical Mathematics*, 2nd ed., ser. Texts in applied mathematics. Springer Berlin Heidelberg, 2007, vol. 37.